2006

Formation and maintenance of shear zones

Caleb Holyoke, *University of Akron*
Jan Tullis, *Brown University*

Formation and maintenance of shear zones

Caleb W. Holyoke, III
Jan Tullis
Department of Geological Sciences, Brown University, Providence, Rhode Island 02912, USA

ABSTRACT

The processes that initiate and maintain prograde ductile shear zones are not well understood. We have performed shear experiments (γ = 1 to 3) on a fine-grained (100–150 μm) gneiss (59% quartz, 28% plagioclase, 13% aligned but not interconnected biotite) to determine the evolution of deformation mechanisms that produce dramatic strain weakening and localization, at conditions (1.5 GPa, 800 °C, $\dot{\gamma} = 2 \times 10^{-5}$/s) where pure quartz aggregates deform homogeneously by dislocation creep. Initial yield occurs where stress concentrations at the tips of weak biotite grains produce semibrittle deformation in intervening quartz or plagioclase, allowing local biotite interconnection by slip on (001) and initiating strain weakening. After yield, the interconnected biotites kink and thus strengthen, but the highly strained parts of grains react to a fine-grained, mixed-phase assemblage which deforms by grain-size–sensitive creep, allowing further strain weakening and localization. At γ = 3.3, the strain and strain rate in the ~100-μm-thick shear zone are 100 times that of the enclosing host rock, similar to the localization observed in natural shear zones. Thus, the processes that initiate strain localization are not necessarily the same as those that preserve the weak shear zone, and once formed, a shear zone may be permanently weakened.

Keywords: shear zones, polyphase processes, biotite gneiss, strain localization, Gneiss Minuti.

INTRODUCTION

Ductile shear zones are common features in Earth's crust. The localization of strain requires strain weakening, which means a transition from higher-stress to lower-stress deformation mechanisms at a constant strain rate. Therefore, an understanding of the strain-weakening mechanisms that operate in shear zones is critical to determine the strength of the lithosphere. However, the mechanisms that lead to the formation of ductile shear zones are not well understood because the subsequent high strain obliterates the microstructural evidence of their operation. The weakening mechanisms in a polyphase rock, such as a quartzo-feldspathic gneiss, are likely to involve either the interconnection of an initially dispersed weak phase such as mica (e.g., Berthe et al., 1979), formation of weak phases by hydration reactions (e.g., Mitra, 1978), or formation of fine-grained, mixed-phase assemblages that can deform by diffusion-accommodated grain boundary sliding (e.g., Stünitz and Tullis, 2001).

Handy (1990, 1994) has emphasized the importance of the transition from a load-bearing framework to an interconnected weak phase, but the specific processes by which polyphase aggregates accomplish such a transition at conditions where the framework minerals deform by crystal plasticity are not well understood. Similarly, the feedbacks between high strain and metamorphic reactions are not well understood, although reactions restricted to shear zones are commonly documented (e.g., Keller et al., 2004). We undertook an experimental study to determine how these two important processes act to initiate and maintain a localized ductile shear zone. Shear experiments at several different strains allowed us to observe the evolution of deformation mechanisms during the strain weakening that accompanied the transition from a load-bearing framework of quartz to through-going interconnection of the weak phase (biotite), at conditions where the framework phase undergoes dislocation creep. Additionally, due to the high temperatures used in this study, the interconnected, highly strained biotite grains reacted with quartz and plagioclase to form a fine-grained mixed-phase assemblage (garnet, K-feldspar, and water) that maintained the weakness of the materials in the narrow shear zone and allowed it to accommodate the majority of sample strain (Fig. 1B). Our results provide insight to the evolution of stresses and deformation mechanisms operating in a polyphase aggregate, and the factors that allow strain localization to be maintained.

EXPERIMENTAL PROCEDURES

Experiments were conducted using the Gneiss Minuti, a fine-grained (~150 ± 25 μm) quartzo-feldspathic gneiss from the southern Alps (Zurbriggen et al., 1998). All experimental samples were cored from two layers of the gneiss composed of 13 vol% biotite, 28 vol% plagioclase ($An_{27.7}Ab_{71.9}Or_{0.4}$), 58 vol% quartz, and 1 vol% garnet/Fe-Ti oxides (Fig. 1A). Quartz and plagioclase grains are relatively equant and have no optically visible deformation microstructures. Quartz grains form an interconnected framework, biotite grains are well aligned but not interconnected, and plagioclase grains are also isolated.

All experiments were conducted with no added water at 800 °C, 1.5 GPa, and a shear strain rate ($\dot{\gamma}$) = 2×10^{-5}/s. Samples 1.2 mm thick were sliced from cores with the foliation parallel to the shear plane and placed between two 45°-cut Al_2O_3 shear pistons (inset, Fig. 1A). Three samples of Gneiss Minuti were deformed to shear strains (γ) of 0.6 (at yield), 1.1 (during strain weakening), and 3.3 (steady state), with associated thinning of 10%, 17%, and 37%, respectively (Table 1). Experiments were conducted using an all-salt assembly; there is some error in stress (~50 MPa) due to piston friction, but it is considerably less

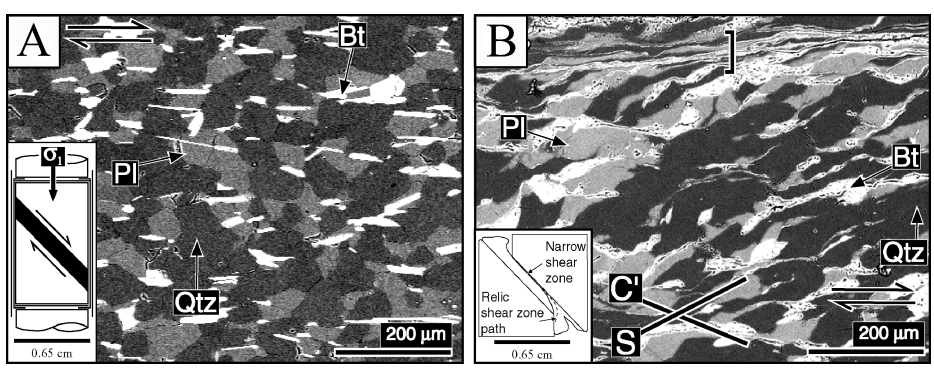

Figure 1. In scanning electron microscope–backscattered electron (SEM-BSE) images, quartz is always darkest gray, plagioclase is intermediate gray, and biotite is white. A: Gneiss Minuti, SEM-BSE micrograph; ~100–150 μm grain size, 55 vol% quartz, 33 vol% plagioclase (An_{30}), 13 vol% biotite. Inset shows schematic of sample and pistons. B: SEM-BSE image of W1008. Narrow shear zone (bracket) accommodates most of sample strain (schematic in inset shows geometry). Abandoned shear zone path indicated by dashed line. S—foliation surface; C—shear surface.

TABLE 1. OPTICAL AND TEM MICROSTRUCTURES OF THREE SAMPLES OF GNEISS MINUTI

Expt.	Shear Strain/ Thinning	Sample scale structure	Optical and TEM Microstructures		
			Quartz	Biotite	Plagioclase
W1019	0.6/10%	Initial interconnection of biotite grains by grain-scale faults in quartz and plagioclase	High density of tangled dislocations away from tips of biotite grains, microcracks and parallel arrays of tangled dislocations near tips of biotite grains. Grain-scale faults through some grains (Fig. 3).	Kinks and some shearing into grain-scale faults through framework grains. (Fig. 3)	Fracturing of grains, few dislocations
W1009	1.1/17%	Strands of multiply interconnected biotite grains, first reaction products, weak S-C′ fabric	High density of tangled dislocations in porphyroclasts and some fine (~1 μm) recrystallized grains at the boundaries.	Kinking, shearing, and a few initial dehydration reaction products (<<1 vol%) in highly strained biotites (Fig. 4)	Fracturing of grains, few dislocations.
W1008	3.3/37%	Single through-going shear zone, weak S-C′ fabric outside of shear zone (Fig. 1b)	In shear zone, very fine-grained and highly recrystallized, outside of shear zone, undulatory extinction, low dislocation density, dislocation arrays, and some fine recrystallized grains (~1–2 μm, Fig. 5)	Inside shear zone, highly sheared partially dehydrated (~30 vol% reaction) intermixed with fine-grained (~1 μm) reaction products (Fig. 5); outside shear zone some kinking, minor shearing and few reaction products (~1 vol%, Fig. 5)	Fracturing of grains, few dislocations.

than the changes in flow stress observed during the experiments (>500 MPa).

Deformed samples were impregnated with epoxy, and thin sections oriented parallel to the XZ plane were prepared for petrographic analysis and scanning electron microscopy (SEM); separate sections were prepared for transmission electron microscopy (TEM). Force-displacement data were corrected for changing area of overlap of the 45°-cut pistons, for thinning of the sample, and for friction within the assembly in order to produce plots of differential stress versus shear strain (Fig. 2).

RESULTS

The stress-strain curves for the Gneiss Minuti samples (Fig. 2) show pronounced strain weakening, with an average peak strength of 1.3 GPa followed by weakening to 40% of the yield strength by $\gamma \approx 3$. The sample-scale and grain-scale microstructures in each sample are listed in Table 1; representative microstructures are illustrated in Figures 1B, 3, 4, and 5.

Quartz forms the interconnected framework in the Gneiss Minuti, and its deformation mechanisms are the most sensitive to stress variations at the experimental conditions. The deformation mechanisms of semibrittle flow and recrystallization- and climb-accommodated dislocation creep, their relation to flow stress, and their microstructures are documented in Hirth and Tullis (1992, 1994). Therefore, quartz microstructures were used to infer changes in deformation processes that accompany strain weakening and localization. Because the biotites are in their weakest easy slip orientation, most of the load is initially borne by the quartz-plagioclase framework. The microstructural variations observed in quartz grains depend on their location relative to biotite grains. In the low-strain, high-stress sample, quartz near the tips of biotite grains deformed by semibrittle flow, whereas away from the tips of biotite grains, it deformed by recrystallization-accommodated dislocation creep (Figs. 3A and 3B). In the high-strain, lower-stress sample, after formation of a throughgoing shear zone that accommodates the majority of strain (Fig. 1B), quartz microstructures indicate a transition from recrystallization- to climb-accommodated dislocation creep.

Although no biotite reaction was observed in cores of Gneiss Minuti held hydrostatically at pressure and temperature for the duration of the longest deformation experiment, some reaction did occur in highly strained biotite grains in the two higher-strain samples. In the mid-strain sample, minor reaction products (≪1 vol% garnet) were observed along the edges of highly strained, interconnected biotite grains (inset, Fig. 4). In the high-strain sample, significant (30 vol%) reaction occurred in the throughgoing shear zone, and the reaction products (primarily garnet) are thoroughly mixed with the remaining biotite.

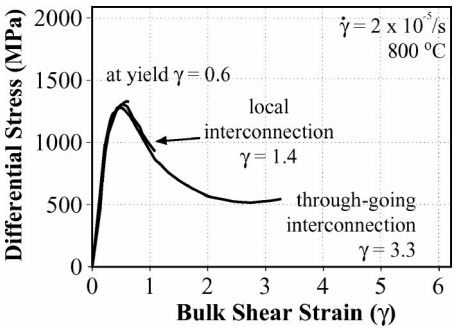

Figure 2. Differential stress versus bulk shear strain.

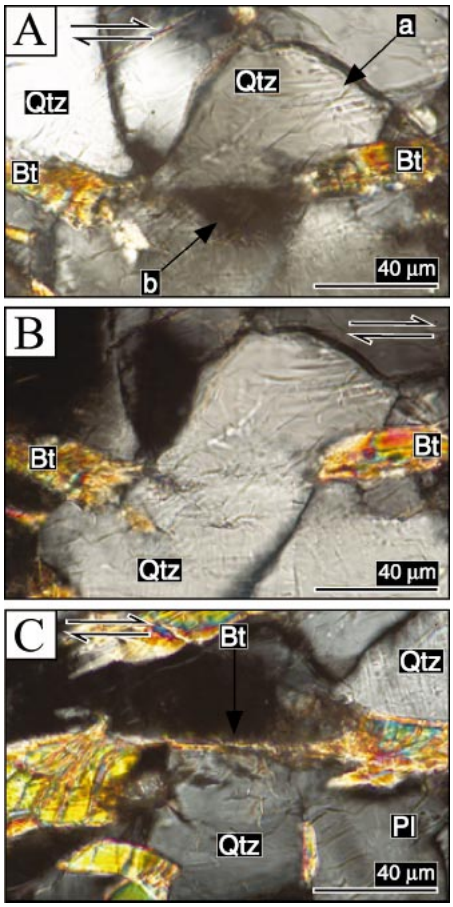

Figure 3. Low-strain sample (W1019) optical micrographs. A: Quartz grain between two biotite grains developed zone of localized strain (area "b," at extinction), whereas away from zone, quartz is less deformed (area "a," with deformation lamellae). B: Same as A, but polarizers rotated 45°. C: Biotite lining grain-scale shear zone in quartz formed in response to local stress concentrations between two biotite grains.

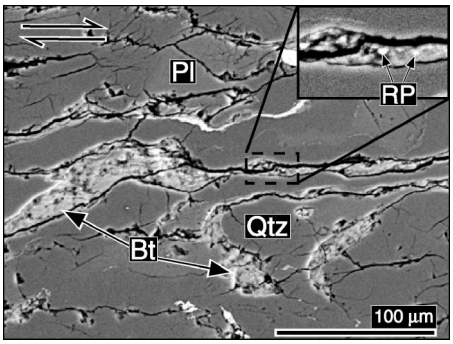

Figure 4. Scanning electron microscope–secondary electron image of mid-strain sample (W1009). Quartz and plagioclase are similar medium gray; biotite is light gray. Sheared biotite grains and dehydration reaction products (RP, enlarged in inset) observed only in highly strained biotite; no reaction occurred in undeformed portion of biotite grain.

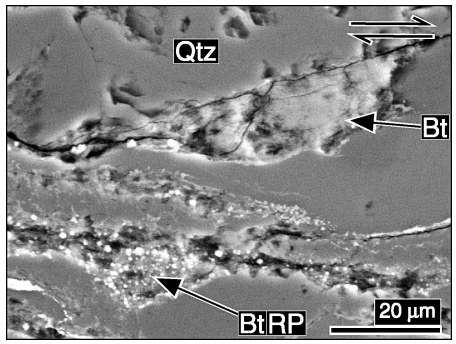

Figure 5. Scanning electron microscope–secondary electron image of high-strain sample (W1008). Quartz and plagioclase are similar medium gray; biotite is lightest gray. Image shows shear zone (lower half of image); biotite grain (Bt) adjacent to shear zone is partially reacted (Bt/RP) where highly strained.

However, very little reaction occurred in biotite grains outside the shear zone (Fig. 5). The reaction forming the mixed-phase assemblage in the shear zone is 2 Bt + 3 An + 3 Qtz ⇔ 3 almandine/pyrope + grossular + 2 K-feldspar + 2 H_2O. The details of the reaction and stability field are not pertinent to this study; they are discussed in more detail in a separate study.

DISCUSSION

Shear Zone Formation: Weak Phase Interconnection

The initial biotite interconnection occurred by (001) slip in a few locations where intervening quartz underwent grain-scale faulting. The localized semibrittle flow microstructures observed in quartz at the tips of biotite grains indicate that the stresses there are significantly higher than elsewhere; Hirth and Tullis (1994) found that stresses of 1.6–2.3 GPa were required for semibrittle flow of quartzites at the P, T, and $\dot{\gamma}$ of our experiments. These values are consistent with models of the stress distribution in an elastic sheet containing weak ellipsoidal inclusions with an aspect ratio of 5:1 (similar to the biotite grains in the Gneiss Minuti) and oriented at 45° to σ_1, which predict stress concentrations 1.5 times the remote stress, or ~2 GPa for our samples at yield (Jaeger and Cook, 1969). These results are also similar to those of Johnson et al. (2004), who modeled the stress concentrations in a hard matrix at the tips of weak zones with an aspect ratio similar to that of our micas, and found them to be ~1.3–2 times the confining pressure. Similar localized deformation resulting from stress concentrations near biotite grains was observed in quartzo-feldspathic gneiss samples deformed at lower P-T conditions where the matrix quartz and feldspar grains are entirely brittle (e.g., Gottschalk et al., 1990).

In the Gneiss Minuti samples, initial interconnection of biotite grains increases the aspect ratio of the weak inclusion, thus increasing the stress concentration at its tip and promoting further interconnection to additional biotite grains. However, as these interconnected biotite grains slip, they begin to kink, due to the highly heterogeneous stress and strain distribution in the samples. Kinking rotates portions of the grains away from the easy slip orientation into a hard orientation (Kronenberg et al., 1990). This strengthening of biotite grains decreases the stress concentrations within the adjacent quartz-plagioclase framework, and it partitions strain to weaker, unkinked biotite grains, requiring a different mechanism to keep the incipient shear zone weak and localized.

Shear Zone Maintenance

In nature, dynamic recrystallization of new strain-free biotite grains serves to remove kinked grains and prevent strain hardening in narrow mica-rich ductile shear zones (e.g., Berthe et al., 1979; Gapais, 1989). However, at the high temperature of this study, portions of biotite grains that become highly strained undergo dehydration reaction (Figs. 4 and 5). The enhanced reaction kinetics in highly strained grains are due to the increased surface area for nucleation and the higher internal strain energy, as also observed by Stünitz and Tullis (2001).

The localization of the biotite reaction within the ductile shear zone serves to further weaken the shear zone in two ways. First, it creates a fine-grained (1–3 μm) mixture of product phases (garnet, K-feldspar) that are dislocation free and thoroughly mixed with fine-grained biotite, allowing a switch to diffusion-accommodated grain boundary sliding. Second, the water released by 30% reaction of the biotite in the shear zone is ~0.2 wt% of the quartz and plagioclase within the shear zone, an amount demonstrated to cause hydrolytic weakening of quartz (Hirth and Tullis, 1992). The combination of localized reaction-induced grain boundary sliding and hydrolytic weakening allows strain to continue to be localized in a single narrow shear zone (Figs. 1B and 5). Although the specific reaction observed in this study is not common in Earth's crust, its effects are identical to those observed in natural zones of reaction-induced strain localization (Keller et al., 2004).

Evolution of Strain and Strain Rate During Strain Localization

We have estimated the difference in strain and strain rate between the shear zone and the material outside the shear zone (''host rock'') using quartz microstructures in the intermediate- and high-strain samples. The orientations of the long axes of quartz porphyroclasts relative to the shear plane were measured in the intermediate-strain sample and in the host rock portion of the high-strain sample. The difference in flattening (pure shear) between the two samples was removed, and the shear strain between the two samples was calculated to be $\gamma = 0.3$. The strain rate of the host rock portion of the high-strain sample was then calculated from the time difference between the two experiments. The samples followed the same stress-strain path, and the thickness of the host rock in the high-strain sample is known, so its shear strain rate (3.0×10^{-6}/s) could be calculated. The strain rate of the shear zone (2.8×10^{-4}/s) could then be calculated because the sum of the host rock and shear zone strain rates times their respective volume fractions must equal the bulk shear strain rate (2.3×10^{-5}/s). This relationship also allowed us to calculate the shear strain in the shear zone ($\gamma = 30$). A schematic diagram of the evolution of quartz deformation mechanisms and strain rates prior to and after localization is presented in Figure 6.

We can check the calculated strain rates for the host rock and the shear zone in the high-strain sample by comparing the quartz microstructures in the two regions with those observed by Hirth and Tullis (1992) in pure quartzites deformed at the same P and T. In quartz grains within the host rock, with a calculated strain rate of 3.0×10^{-6}/s, we observe some dislocation arrays and some very small dislocation-free recrystallized grains, consistent with dislocation creep that is transitional between recrystallization- and climb-accommodated. For a strain rate of 3.0×10^{-6}/s at 800 °C, Hirth and Tullis (1992) observed that ''as-is'' quartzites deform by dislocation creep that is transitional between re-

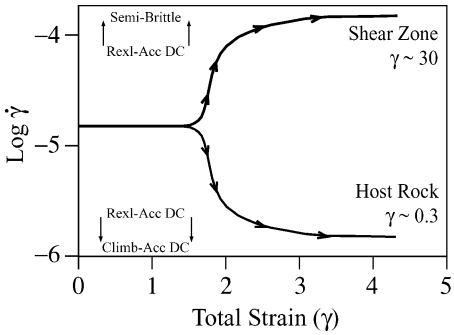

Figure 6. Shear strain rate versus bulk shear strain. After shear zone develops, finite strain and strain rate within shear zone and host rock differ by two orders of magnitude. Approximate deformation mechanism transitions in quartzites for experimental conditions: Semibrittle—semibrittle flow; Rexl-Acc DC—recrystallization-accommodated dislocation creep; and Climb-Acc DC—climb-accommodated dislocation creep.

crystallization- and climb-accommodated. Quartz grains within the shear zone, with a calculated strain rate of 2.8×10^{-4}/s, include porphyroclasts with a high dislocation density but no cracks and small dislocation-free recrystallized grains, consistent with recrystallization-accommodated dislocation creep. However, the results of Hirth and Tullis (1992, 1994) indicate that water-added quartzite at this strain rate should deform by semibrittle flow. This apparent contradiction indicates that even within the exceedingly narrow ductile shear zone, strain and strain rate are partitioned away from the quartz grains and into the mixed-phase reaction products.

Comparison to Natural Shear Zones

In our gneiss samples that develop strain localization and weakening, we observe a sequence of quartz microstructures indicative of decreasing stress. The same sequence of stress-dependent microstructures is observed in natural quartzites (e.g., Dunlap et al., 1997; Stipp et al., 2002). Strain weakening indicates a transition from higher- to lower-stress deformation mechanisms during constant strain rate deformation. The high-stress deformation mechanisms that initiate strain localization in our samples are replaced by lower-stress mechanisms after strain weakening and localization. In nature, the microstructures produced by the higher-stress localization mechanisms during shear zone formation will most likely be overprinted by the microstructures of the subsequent lower-stress deformation mechanisms, as was observed in the host rock portion of our high-strain sample. Therefore, the only location in a natural shear zone that may preserve microstructures indicative of shear zone initiation processes will be the tip of the shear zone where it terminates, and even there evidence of the high-stress mechanisms may have been obliterated by later annealing.

As long as a significant difference in strength exists between phases in any rock, it is likely that the isolated weak phase will become interconnected, causing strain localization. Studies of natural shear zones infer the formation of weak zones to have resulted from the interconnection of weaker minerals, such as micas or quartz in granites with a feldspar framework (e.g., Berthe et al., 1979; Gapais, 1989; Lonka et al., 1998; Johnson et al., 2004); or a retrograde reaction to inherently weak material such as micas (Mitra, 1978); or the formation of fine-grained mixed-phase reaction products (Keller et al., 2004). In each case, processes such as dynamic recrystallization or grain boundary sliding prevent the localized weak material from strengthening.

IMPLICATIONS

The similarity of the microstructures and degrees of strain and strain rate partitioning observed in the microscale shear zone in our sample to those observed in natural mesoscale (e.g., Keller et al., 2004) and megascale (e.g., Norris and Cooper, 2003) shear zones is striking and suggests that our results scale well to natural processes. Our results suggest several general implications for the deformation of natural rocks.

- The higher-stress deformation mechanisms that initiate ductile shear zones are not the same as the lower-stress deformation mechanisms operating after localization and are not preserved after small strains.
- The restriction of reaction products to high-strain zones indicates that high strain enhances reaction progress.
- In order to maintain strain localization, additional processes may be required to preserve the weakness of the material in the shear zone.
- Once formed, the localized weak zone will remain weaker than the adjacent host rock, and in subsequent deformation events, strain will tend to relocalize in the weak zone, even if it is not in the optimal orientation.

ACKNOWLEDGMENTS

This work was supported by a National Science Foundation grant to Tullis (EAR-0208150). We would like to thank P. Gromet and the journal reviewers (J. Selverstone, A. Kronenberg, and S. Johnson) for their comments and B. Collins for thin sections.

REFERENCES CITED

Berthe, D., Choukroune, P., and Jegouzo, P., 1979, Orthogneiss, mylonite and non coaxial deformation of granites: The example of South Armorican shear zone: Journal of Structural Geology, v. 1, p. 31–42, doi: 10.1016/0191-8141(79)90019-1.

Dunlap, W.J., Hirth, G., and Teyssier, C., 1997, Thermomechanical evolution of a ductile duplex: Tectonics, v. 16, p. 983–1000.

Gapais, D., 1989, Shear structures within deformed granites: Mechanical and thermal indicators: Geology, v. 17, p. 1144–1147, doi: 10.1130/0091-7613(1989)017<1144:SSWDGM>2.3.CO;2.

Gottschalk, R.R., Kronenberg, A.K., Russell, J.E., and Handin, J., 1990, Mechanical anisotropy of gneiss: Failure criterion and textural sources of directional behavior: Journal of Geophysical Research, v. 95, p. 21,613–21,634.

Handy, M.R., 1990, The solid-state flow of polymineralic rocks: Journal of Geophysical Research, v. 95, p. 8647–8661.

Handy, M.R., 1994, Flow laws for rocks containing two non-linear viscous phases: A phenomenological approach: Journal of Structural Geology, v. 16, p. 287–301, doi: 10.1016/0191-8141(94)90035-3.

Hirth, G., and Tullis, J., 1992, Dislocation creep regimes in quartz aggregates: Journal of Structural Geology, v. 14, p. 145–159, doi: 10.1016/0191-8141(92)90053-Y.

Hirth, G., and Tullis, J., 1994, The brittle-plastic transition in experimentally deformed quartz aggregates: Journal of Geophysical Research, v. 99, p. 11,731–11,748, doi: 10.1029/93JB02873.

Jaeger, J.C., and Cook, N.G.W., 1969, Fundamentals of rock mechanics: London, Chapman and Hall, 515 p.

Johnson, S., Vernon, R., and Upton, P., 2004, Foliation development and progressive strain-rate partitioning in the crystallizing carapace of a tonalite pluton: Microstructural evidence and numerical modeling: Journal of Structural Geology, v. 26, p. 1845–1865, doi: 10.1016/j.jsg.2004.02.006.

Keller, L.M., Abart, R., Stuenitz, H., and De, C.C., 2004, Deformation, mass transfer and mineral reactions in an eclogite facies shear zone in a polymetamorphic metapelite (Monta Rosa nappe: western Alps): Journal of Metamorphic Geology, v. 22, p. 97–118, doi: 10.1111/j.1525-1314.2004.00500.x.

Kronenberg, A.K., Kirby, S.H., and Pinkston, J., 1990, Basal slip and mechanical anisotropy of biotite: Journal of Geophysical Research, v. 95, p. 19,257–19,278.

Lonka, H., Schulmann, K., and Venera, Z., 1998, Ductile deformation of tonalite in the Suomusjarvi shear zone, southwestern Finland: Journal of Structural Geology, v. 20, p. 783–798, doi: 10.1016/S0191-8141(98)00003-0.

Mitra, G., 1978, Ductile deformation zones and mylonites: The mechanical processes involved: American Journal of Science, v. 278, p. 1057–1084.

Norris, R.J., and Cooper, A.F., 2003, Very high strains recorded in mylonites along the Alpine fault, New Zealand: Journal of Structural Geology, v. 25, p. 2141–2157, doi: 10.1016/S0191-8141(03)00045-2.

Stipp, M., Stuenitz, H., Heilbronner, R., and Schmid, S.M., 2002, The eastern Tonale fault zone; a ''natural laboratory'' for crystal plastic deformation of quartz over a temperature range from 250 to 700 degrees C: Journal of Structural Geology, v. 24, p. 1861–1884.

Stünitz, H., and Tullis, J., 2001, Weakening and strain localization produced by syn-deformational reaction of plagioclase: International Journal of Earth Sciences, v. 90, p. 136–148, doi: 10.1007/s005310000148.

Zurbriggen, R., Kamber, B.S., Handy, M.R., and Naegler, T.F., 1998, Dating synmagmatic folds: A case study of Schlingen structures in the Strona-Ceneri Zone (southern Alps, northern Italy): Journal of Metamorphic Geology, v. 16, p. 403–414, doi: 10.1111/j.1525-1314.1998.00145.x.

Manuscript received 31 July 2005
Revised manuscript received 10 October 2005
Manuscript accepted 12 October 2005

Printed in USA